

Miniemulsion polymerization of styrene in the presence of a water-insoluble blue dye

C.S. Chern*, T.J. Chen and Y.C. Liou

Department of Chemical Engineering, National Taiwan University of Science and Technology, Taipei 106, Taiwan

(Received 5 August 1997; accepted 18 November 1997)

Relatively stable styrene (ST) miniemulsions were prepared by using a water-insoluble, low molecular weight blue dye as the cosurfactant. The data of the monomer droplet size, creaming rate and phase separation of the monomer as a function of time, were used to evaluate their shelf stability. The dye concentration in toluene can be determined by UV absorbance at 678 nm. This makes the dye molecule a potential probe for determining the loci of particle nucleation during miniemulsion polymerization. In the subsequent miniemulsion polymerization, latex particles were produced via both the monomer droplet nucleation and homogeneous nucleation. Approximately 60% of the original monomer droplets was successfully nucleated during polymerization based on the data of the weight percentage of dye incorporated into the final latex particles (P_{dye}). The parameter P_{dye} goes up with increasing [dye] (0.1% → 1.0% based on total monomer), which is attributed to the increased resistance against diffusional degradation of the monomer droplets. This may greatly reduce the number of primary particles nucleated in the aqueous phase and, thereby, increase the degree of incorporation of dye into the final latex particles. Conductivity measurements during polymerization also support the mixed modes of particle nucleation.
 © 1998 Published by Elsevier Science Ltd. All rights reserved.

(Keywords: miniemulsion polymerization; styrene; water-insoluble dye)

INTRODUCTION

In the past 50 years, several particle nucleation mechanisms have been proposed for the conventional emulsion polymerization. These mechanisms include micellar nucleation^{1–3}, homogeneous nucleation^{4–6} and coagulative nucleation^{7,8}. Monomer-swollen micelles (~10¹ nm in diameter, 10²⁰–10²¹ micelles per liter water) will form in the aqueous phase when the surfactant concentration is above its critical micelle concentration (CMC). Free radical polymerization will start immediately after addition of a water-soluble initiator such as sodium persulfate. After polymerizing with a few monomer molecules, the initiator radicals produced in water may become relatively hydrophobic and then enter the monomer-swollen micelles. Propagation of these oligomeric radicals with monomer will continue to take place inside the micelles. As a result, these micelles will be converted into primary latex particles. The probability for the monomer droplets (> 10³ nm in diameter, 10¹³–10¹⁴ monomer droplets per liter water) to capture free radicals from the aqueous phase is insignificant. This is because the total monomer droplet surface area is much smaller than the micelle–water interfacial area. Such a particle formation process is termed the micellar nucleation mechanism. However, both the homogeneous and coagulative nucleation mechanisms propose that the polymer reaction taking place in the aqueous phase should play an important role in the nucleation of latex particles. The function of surfactant is only to stabilize the primary latex particles nucleated in water. For example, according to the homogeneous nucleation mechanism, oligomeric radicals generated in water become insoluble when a critical

chain length is achieved. This water-insoluble radical may thus coil up and form a particle nuclei (~10⁰ nm in diameter). Subsequently, primary particles (~10¹ nm in diameter) are produced via limited flocculation among the unstable particle nuclei and adsorption of surfactant on the newly created particle surfaces. In general, the particle nucleation period is quite short in batch emulsion polymerization, but it has a significant influence on the final latex particle size and size distribution. Control of the latex particle size and size distribution is crucial in determining the quality of latex products. Further information on this subject can be found in Refs^{9,10}.

Miniemulsion polymerization^{11–23}, however, refers to a quite different scenario that both the particle nucleation and subsequent propagation reaction occur primarily in the submicron monomer droplets. This polymerization technique involves dispersion of a large number of homogenized monomer droplets [e.g. styrene (ST)] in water at the reaction temperature with the aid of surfactant (e.g. sodium dodecyl sulfate, SDS)/cosurfactant [e.g. low molecular weight hexadecane (HD) or cetyl alcohol (CA)], followed by addition of the persulfate initiator solution. These monomer droplets may remain stable during polymerization by using a surfactant to prevent coalescence among the interactive droplets in combination with a cosurfactant to retard diffusion of monomer from small droplets to large droplets (Ostwald ripening)²⁴. Furthermore, these tiny monomer droplets have an extremely large droplet surface area and, therefore, they may compete effectively with the monomer-swollen micelles for the oligomeric radicals generated in water. The particle nuclei formed via the homogeneous nucleation or coagulative nucleation (if any) also can be absorbed by these monomer droplets. After capture of the oligomeric radicals from the aqueous phase, the

* To whom correspondence should be addressed. Tel:886227376649; Fax: 886227376644; e-mail: chern@ch.ntust.edu.tw

polymerizing monomer droplets are then transformed into latex particles. The monomer droplets may thus become the predominant loci for polymer particle nucleation.

In our previous report^{25,26} alkyl methacrylates [e.g. dodecyl methacrylate (DMA) and stearyl methacrylate (SMA)] were used as the reactive cosurfactant to prepare stable styrene miniemulsions. Like conventional cosurfactants [e.g. cetyl alcohol (CA) and hexadecane (HD)], alkyl methacrylates may act as a normal cosurfactant in stabilizing the homogenized monomer droplets. Furthermore, the methacrylate group can be chemically incorporated into the latex particles in subsequent miniemulsion polymerization, as shown by the IR spectra. Based on the experimental data of the average size of the monomer droplets for the miniemulsion sample, which were taken immediately before the start of polymerization, the average size of latex particles/monomer droplets for the latex samples taken during polymerization and the final latex particle size and size distribution, showed that the miniemulsion polymerization with more hydrophobic SMA or HD had a predominant monomer droplet nucleation. The resulting particle size distribution was relatively narrow. Approximately 80% of the original monomer droplets were successfully nucleated and the remaining droplets only served as the monomer reservoir during polymerization. On the other hand, polystyrene latex particles were produced via both the monomer droplet nucleation and homogeneous nucleation in the miniemulsion polymerization using the less hydrophobic DMA or CA as the cosurfactant. This resulted in a quite broad particle size distribution. However, the fraction of the monomer droplets that had participated in the particle formation process was not determined due to the mixed modes of particle nucleation.

The blue dye (Blue 70, provided by Shenq-Fong Fine Chemical Ltd, China) has a molecular structure shown in Figure 1. The dye has a molecular weight of about 1×10^3 g/mol and it is sparingly soluble in water. The hydrophobic dye may thus represent a candidate for effectively retarding the Ostwald ripening effect during the miniemulsion polymerization. Also the dye concentration in a nonpolar solvent such as toluene can be determined by UV absorbance at 678 nm. These unique properties make the dye molecule a potential probe for determining the loci of particle nucleation during miniemulsion polymerization. Conductivity measurements during polymerization were also used to monitor the particle nucleation process according to Reimers and Schork²⁷. The objective of this work was therefore to study the feasibility of using the water-insoluble dye to determine the fraction of the monomer droplets that can be ultimately nucleated if both the monomer droplet nucleation and homogeneous nucleation mechanisms are operative in the STY miniemulsion polymerization.

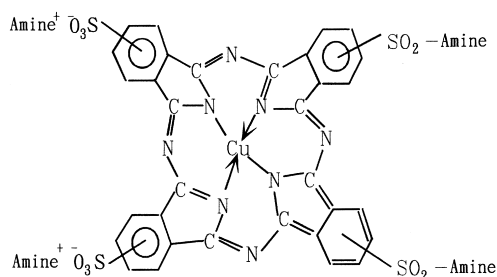


Figure 1 Molecular structure of the dye (Blue 70)

EXPERIMENTAL

Materials

The chemicals used in this work include styrene (Taiwan Styrene Co.), sodium dodecyl sulfate (J. T. Baker), water-insoluble blue dye (Blue 70, Shenq-Fong Fine Chemical Ltd, China), sodium persulfate (Riedel-de Haen), sodium bicarbonate (Riedel-de Haen), toluene (Acros), nitrogen (Ching-Feng-Harg Co.) and deionized water (Barnsted, Nanopure Ultrapure Water System, specific conductance $< 0.057 \mu\text{S cm}^{-1}$). Styrene was distilled under reduced pressure before use. All other chemicals were used as received.

Preparation of ST miniemulsions

The miniemulsion was prepared by dissolving SDS in water and the blue dye in the monomer. The oily and aqueous solutions were mixed with a typical mechanical agitator operated at 400 rpm for 10 min. The resultant emulsion was then homogenized by the Microfluidizer-110Y (Microfluidics Co.), operated at 5000 psi outlet pressure and 10 passes. The shelf-life of the miniemulsion was monitored by placing about 20 ml sample in a capped glass vial at 35°C for one month. The position of the creaming line from the bottom of the sample and the time necessary for a visible monomer phase on the top of the sample to appear were then recorded.

Polymerization process

Polymerization was carried out in a 250 ml reactor equipped with a four-bladed fan turbine agitator, a thermometer, a conductivity meter (Orion Model 115) and a reflux condenser. Immediately after homogenization, the resultant miniemulsion was charged into the reactor and then purged with N₂ for 10 min while the reactor temperature was brought to the reaction temperature. A typical miniemulsion charge comprises 160 g water, 0.0358 g sodium bicarbonate (2.66 mM based on total water), 0.230 g SDS (5 mM based on total water), 0.0400 g dye (0.1 wt% based on total monomer) and 40 g ST. The reaction was then initiated by addition of the initiator solution comprising 5 g water and 0.105 g sodium persulfate (2.66 mM based on total water). The polymerization temperature and agitation speed were kept constant at 80°C and 400 rpm, throughout the reaction (reaction time = 4 h). The theoretical solid content of the latex product is approximate 20%.

Determination of monomer droplet size (or latex particle size)

The data of the average monomer droplet size (or latex particle size) were obtained from the dynamic light scattering method (Otsuka Photal LPA-3000/3100). The sample was diluted with water to adjust the number of photons counted per sec (cps) to 8000–12000. The dilution water was saturated with SDS and ST, prohibiting the diffusion of surfactant and monomer molecules from the monomer droplets (or monomer-swollen latex particles) into water. The reported data represents an average of at least three measurements and the errors have been estimated to be 8% or less.

Characterization of latex products

The latex product was filtered through 40-mesh (0.42 mm) and 200-mesh (0.074 mm) screens in series to collect the filterable solids. Scraps adhering to the agitator,

thermometer and reactor wall were also collected. Total solid content and conversion of styrene as a function of time were determined by the gravimetric method.

A distinct peak at 678 nm was observed for the solution of 1.7×10^{-4} g blue dye and 0.2 g dried polystyrene in 20 ml toluene by the UV absorbance method (Shimadzu, UV-160A). However, no absorbance was detected at this wavelength for the solution of 0.2 g dried polystyrene in 20 ml toluene. Thus, the presence of polystyrene in the sample does not effect UV absorbance of the blue dye at 678 nm. Figure 2 shows the calibration curve of the UV absorbance at 678 nm versus the dye concentration ([dye]) data and the extinction coefficient is determined to be 8.2765×10^4 ml/cm/g. To determine the amount of dye incorporated into the latex particles, the latex product was allowed to stand at room temperature over 3 days before UV absorbance measurements. In this manner, a thin layer of blue precipitate (originated from the bulk dye suspended in the latex product) can be found on the bottom of the sample. Approximately 2 g of sample was pipetted from the middle portion of the latex sample and then dried in an oven. Subsequently, the dried polymer particles was dissolved in 20 ml toluene for determination of the dye content according to the above calibration curve.

RESULTS AND DISCUSSION

Shelf stability of ST miniemulsions prepared by SDS/dye

The solubility of monomer in water increases with decreasing monomer droplet diameter according to the following equation²⁴:

$$C(d_m) = C(\infty)\exp[4\sigma V_m/(RTd_m)] \quad (1)$$

where $C(d_m)$ and $C(\infty)$ are the solubility of monomer in water when the monomer droplet size is d_m and the solubility of the bulk monomer in water, respectively. The parameter σ is the monomer droplet–water interfacial tension, V_m is the molar volume of the substance in the monomer

droplet, R is the gas constant and T is the absolute temperature. This chemical potential effect arising from the monomer droplets with different radii of curvature will cause monomer molecules in the smaller droplets to dissolve in water, diffuse through the aqueous phase, and then enter the larger ones. As a consequence, larger monomer droplets tend to grow in size at the expense of smaller ones and ultimately, this diffusional degradation process will destabilize the miniemulsion (Ostwald ripening). Adequate emulsion stability during storage or polymerization can be achieved by using a water-insoluble, low molecular weight cosurfactant (e.g. CA, HD, DMA and SMA) to retard the monomer diffusion from the small droplets to large ones (osmotic pressure). According to the extended Lifshitz–Slyozov–Wagner (LSW) theory, the rate of Ostwald ripening $[d(d_m^3)/dt]$ for the ST miniemulsion containing a cosurfactant can be predicted by the following equation²⁴:

$$d(d_m^3)/dt = 64\sigma D_{co} V_m C_{co}(\infty)/(9RT\phi_{co}) \quad (2)$$

where t is time, D_{co} is the molecular diffusivity of cosurfactant in water, $C_{co}(\infty)$ is the solubility of the bulk cosurfactant in water and ϕ_{co} is the volume fraction of cosurfactant in the monomer droplet.

Figure 3(a) shows the average monomer droplet size (d_m) data as a function of time (t) for the ST miniemulsions prepared by 5 mM SDS and various levels of [dye] (0.1%–1.0%) upon aging at 35°C. The experimental data are quite scattered, which is probably due to the significant Ostwald ripening effect. This factor might make the task of measuring d_m more difficult. The parameter d_m increases gradually and then levels off for these miniemulsions. This is because the initial monomer droplet size distribution is relatively broad. Thus, the monomer in small droplets tends to diffuse into water and then into large droplets because the water solubility of monomer in the monomer droplets increases with decreasing droplet size (see equation (1)). This leads to a gradual increase in d_m with time. Ostwald

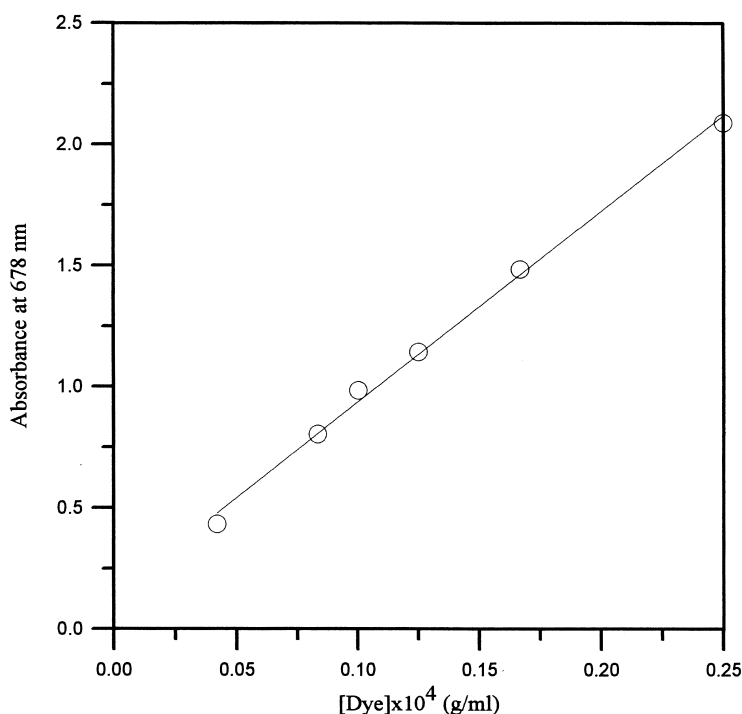


Figure 2 Calibration curve of the UV absorbance at 678 nm versus dye concentration data

ripening is counterbalanced by the osmotic pressure built up later in the aging process and, as a result, d_m approaches a steady value. The steady state value of d_m decreases from 1158 to 897 nm when [dye] increases from 0.1% to 1.0%. In addition, the initial d_m data (378 ± 38 nm) seem insensitive to changes in [dye]. This is due to the same SDS concentration and homogenization condition used in this series of experiments. The slightly scattered data is caused by different rates of Ostwald ripening. These general features were also observed for the ST miniemulsions containing CA or DMA^{25,26}. According to equation (2), the d_m^3 versus t data are shown in Figure 3b. The slope of the least-squares-best-fitted d_m^3 versus t data (i.e. the Ostwald ripening rate) decreases from 3.00×10^6 to 1.64×10^6 nm³/min when [dye] increases from 0.1% to 1.0%. This trend is consistent with equation (2), which predicts that the Ostwald ripening rate is inversely proportional to ϕ_{co} . However, this range of Ostwald ripening rate is much greater than that of miniemulsion stabilized by 5 mM SDS/20 mM CA (1.45×10^5 nm³/min) or 5 mM SDS/20 mM DMA (6.46×10^4 nm³/min)²⁸. This result suggests that the blue dye can be used as a cosurfactant to retard the diffusional degradation of monomer droplets. Nevertheless, it is apparently not as effective as the cosurfactants CA and DMA. One possible explanation is that the blue dye is less hydrophobic than CA or DMA (see Figure 1). In addition, the molecular weight of the blue dye (ca. 1×10^3 g/mol) is much greater than that of CA (242 g/mol) or DMA (254 g/mol). The higher the cosurfactant molecular weight, the less effective is the cosurfactant in promoting the swelling of these monomer droplets (i.e. the smaller is the osmotic pressure effect).

The creaming data for the ST miniemulsions aged at 35°C are shown in Figure 4. The ordinate represents the position of the creaming line from the bottom of the sample. According to the Stokes equation, the creaming rate should be proportional to the square of the monomer droplet size. The miniemulsions, with various levels of [dye] (0.1–1.0%) exhibit significant creaming, owing to the strong Ostwald ripening effect mentioned above. The greater the degree of Ostwald ripening, the larger the resultant monomer droplets. In addition, the early creaming rate data (from 0 to 10 h) is relatively insensitive to changes in [dye]. On the other hand, the extent of Ostwald ripening decreases with increasing [dye] when the aging time is greater than 10 h. A separate monomer phase on the top of the sample was not observed for these miniemulsions over an observation period of 24 h. It should be noted that the creaming phenomenon may not occur during the subsequent miniemulsion polymerization because of the adequate mixing provided by a mechanical agitator.

ST miniemulsion polymerizations stabilized by SDS/dye

First, a conventional emulsion polymerization was carried out to study the mass transfer of the blue dye from the aqueous phase to the growing latex particles. The reaction mixture comprising 2.66 mM NaHCO₃, 5 mM SDS, 24.24% ST based on total water and 2.66 mM Na₂S₂O₈ was polymerized at 80°C for 30 min and the monomer conversion (X) achieved at this point of time was 32.4%. Subsequently, 0.1% dye was added to the reactor and the reaction was allowed to proceed to completion (total reaction time = 4 h, final monomer conversion (X_f) = 94.0% and final latex particle size ($d_{p,f}$) = 84 nm). Note that the SDS concentration used in this series of experiments is below its critical micelle concentration (CMC = 8.2 mM)²⁹.

Thus, the probability of solubilizing the dye molecules in the micelles is very small. Therefore, the amount of dye that can be incorporated into the nucleated micelles is insignificant. As expected, P_{dye} was determined to be only 0.5%. This result implies that transport of the dye molecules from the bulk phase, across the aqueous phase and then into the reaction loci (latex particles) is insignificant due to the very low water solubility of dye.

The data of the monomer conversion (X), the average latex particle/monomer droplet size (d), and the relative conductivity as a function of time (t) for the ST miniemulsion polymerizations with [dye] = 0.1%–1.0% are shown in Figures 5–7, respectively. Note that monomer droplets may coexist with the latex particles in the reaction system and, hence, the dynamic light scattering data for the latex samples taken during polymerization only represent an average size of the mixture comprising both the latex particles and monomer droplets. The dimensionless relative conductivity is defined as the ratio of the conductivity of the

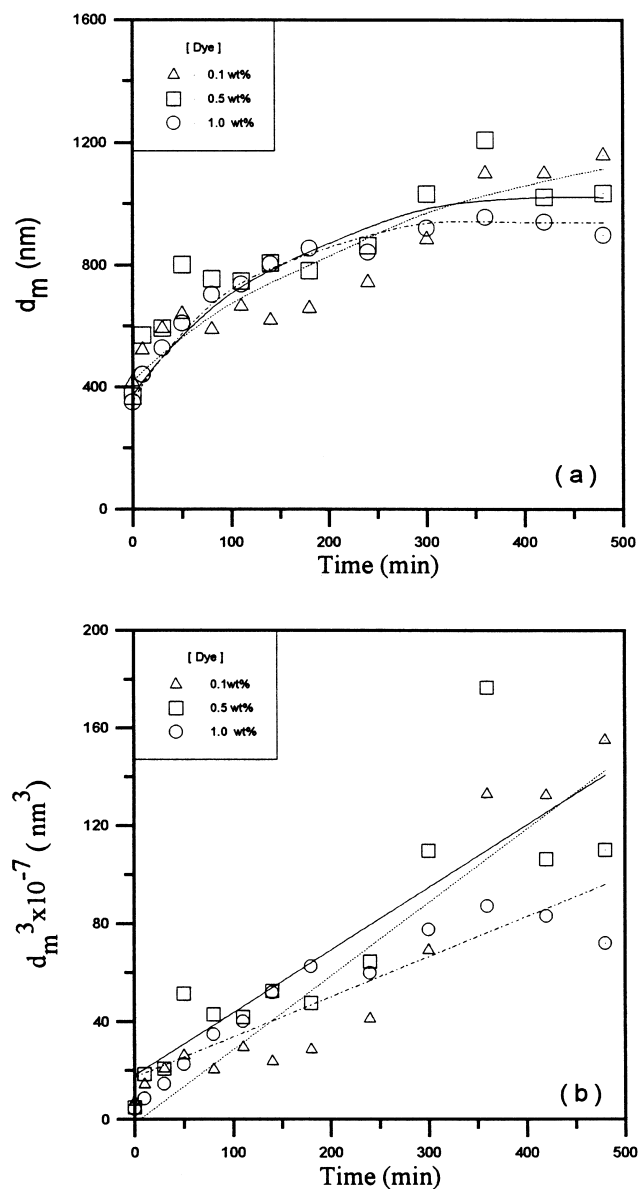


Figure 3 (a) Average monomer droplet size (b) cube of average monomer droplet size as a function of time for the ST miniemulsions stabilized by 5 mM SDS and various levels of dye. [dye] = (Δ , \cdots) 0.1, (\square , ---) 0.5, (\circ , ---) 1.0 wt%

aqueous solution at time t to the conductivity at $t = 0$. The data of the average monomer droplet size at $t = 0$ ($d_{m,i}$), the number of monomer droplets at $t = 0$ ($N_{m,i}$, calculated based on the $d_{m,i}$ data), the final latex particle size ($d_{p,f}$), the

number of final latex particles ($N_{p,f}$, calculated based on the $d_{p,f}$ data), the ratio $N_{p,f}/N_{m,i}$, the final monomer conversion (X_f) and the weight percentage of dye that has been incorporated into the final latex particles (P_{dye}) are also listed in *Table 1*.

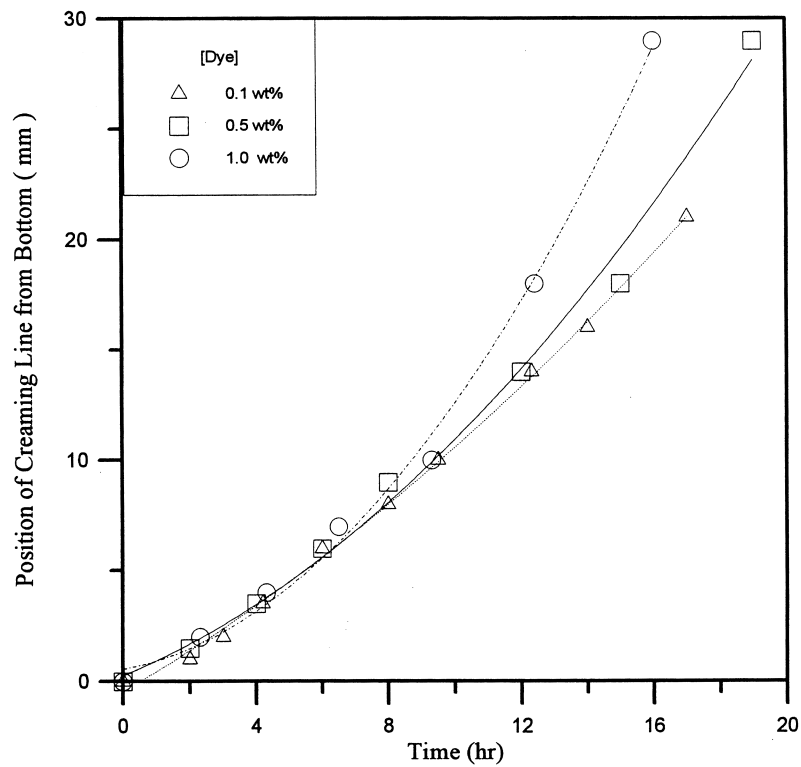


Figure 4 Position of creaming line from the bottom of the ST miniemulsion sample as a function of time. [dye] = (Δ , \cdots) 0.1, (\square , —) 0.5, (\circ , $-\cdot-$) 1.0 wt%

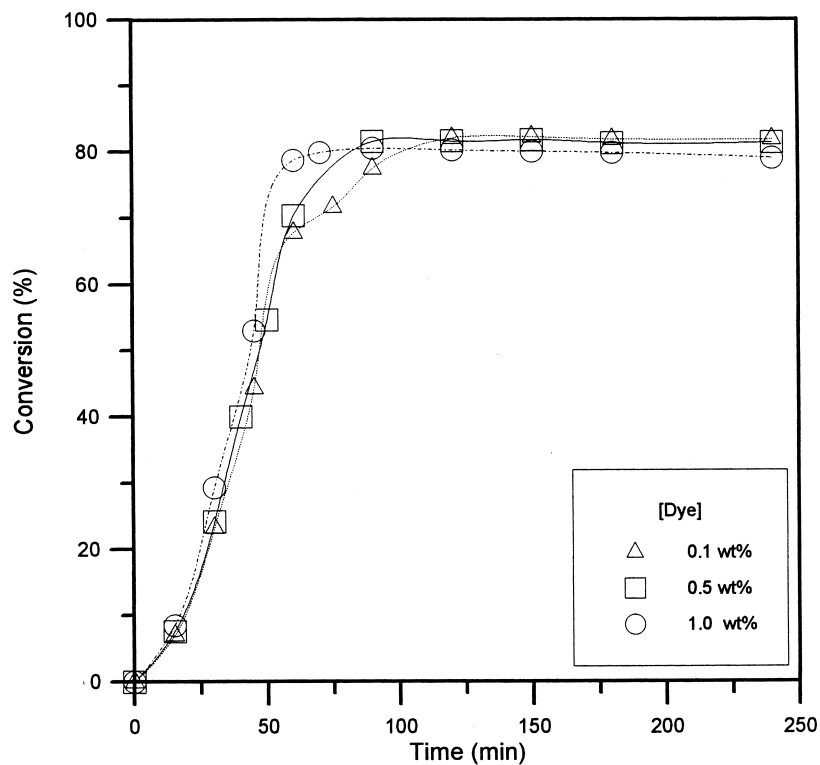


Figure 5 Monomer conversion as a function of time for the ST miniemulsion polymerizations prepared by 5 mM SDS and various levels of dye. [Dye] = (Δ , \cdots) 0.1, (\square , —) 0.5, (\circ , $-\cdot-$) 1.0 wt%

Figures 5 and 6 show that [dye] only has a little effect on both the X versus t and d versus t profiles. For the ST miniemulsion polymerizations stabilized by 5 mM SDS and various levels of [dye] (0.1%–1.0%) at 80°C, the polymerization rate data ($R_p = [M]_0 dX/dt$, determined from the

linear portion of the X versus t curve) fall within the range of 3.26×10^{-2} – 3.58×10^{-2} mol/l/min. The parameter $[M]_0$ represents the initial number of moles of monomer per liter water. As the polymerization proceeds, d decreases rapidly to a minimum, followed by a gradual increase to the plateau.

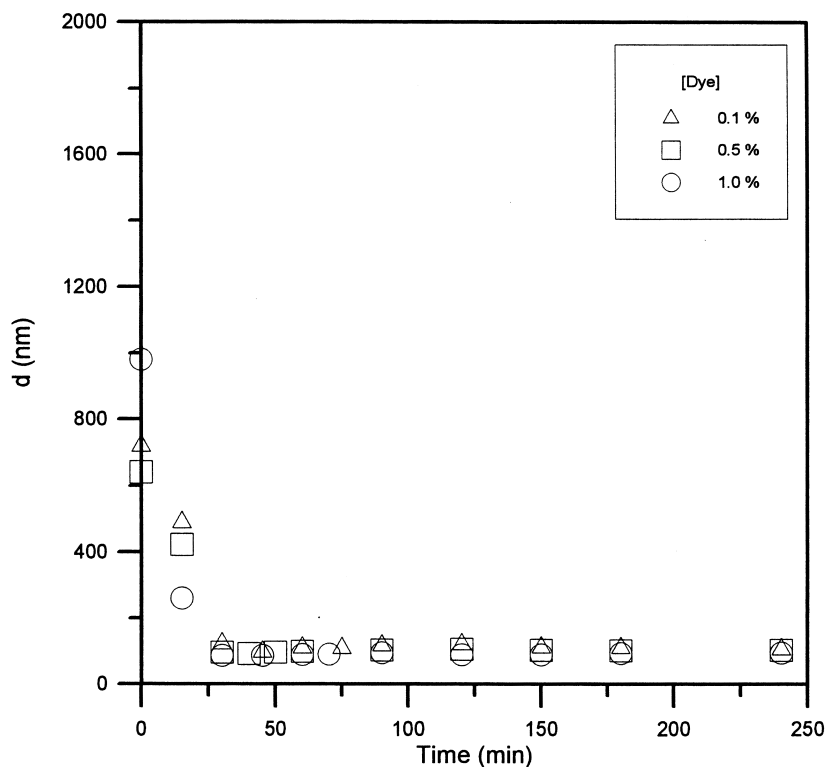


Figure 6 Average latex particle/monomer droplet size as a function of time for the ST miniemulsion polymerizations prepared by 5 mM SDS and various levels of dye. [dye] = (Δ) 0.1, (\square) 0.5, (\circ) 1.0 wt%

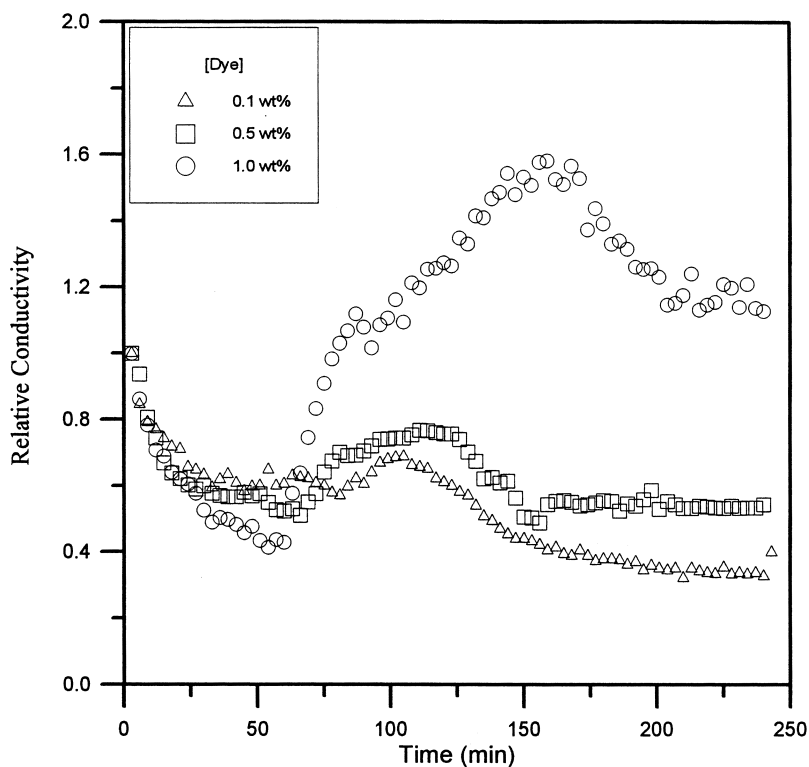


Figure 7 Relative conductivity as a function of time for the ST miniemulsion polymerizations prepared by 5 mM SDS and various levels of dye. [dye] = (Δ) 0.1, (\square) 0.5, (\circ) 1.0 wt%

The rapidly decreased d with t is probably due to the production of particle nuclei by some mechanisms other than monomer droplet nucleation. These particle nuclei are most likely generated by homogeneous nucleation because the SDS concentration is below its CMC. The surfactant required to stabilize these primary particles may come from those dissolved in water, those released from the monomer droplet surfaces due to Ostwald ripening or even those adsorbed on the monomer droplet surfaces. As shown in Figure 3, these ST miniemulsions stabilized by SDS/dye show significant diffusional degradation, which then results in a decrease in the total droplet surface area. The shrinking droplet-water interfacial area may exclude some of the adsorbed SDS species. The desorbed SDS molecules can be adsorbed onto the newly formed particle nuclei and thereby provide these nuclei with electrostatic stabilization. As a result, d decreases significantly during the early stage of polymerization. The parameter $N_{p,f}/N_{m,i}$ is in the range of 189–850 for this series of experiments (see Table 1). This implies that a large proportion of the resultant latex particles are produced by homogeneous nucleation. Table 1 also shows that P_{dye} is in the range of 56%–66%. These data suggest that approximate 56%–66% of the monomer droplets initially present in the reaction system has been successfully converted into latex particles during polymerization. In addition, P_{dye} increases with [dye]. This is reasonable since the larger the amount of dye used in

stabilizing the miniemulsion, the weaker is the Ostwald ripening. This may greatly reduce the number of primary particles nucleated in the aqueous phase and, thereby, increase the degree of incorporation of dye into the final latex particles. Note that the dye molecules originally distributed in the monomer droplets are incapable of diffusing out of these droplets, across the aqueous phase, and then into the latex particles formed by homogeneous nucleation. However, there is no apparent correlation between the two parameters $N_{p,f}/N_{m,i}$ and P_{dye} (see Table 1). The reason for such an inconsistency is not clear at this time, but it is probably related to the errors involved in the calculation of $N_{p,f}$ and $N_{m,i}$.

The reaction mechanism discussed above is further supported by the conductivity data shown in Figure 7. It is shown that the relative conductivity first decreases to a minimum and then increases to a maximum as the polymerization proceeds. This is followed by a reduction in the relative conductivity with t . The decreased conductivity during the early stage of polymerization is attributed to the formation of primary particles in the aqueous phase. These primary particles require adsorption of sufficient surfactant on the newly created particle surfaces in order to maintain adequate colloidal stability. This will rapidly deplete the surfactant molecules dissolved in water. In addition, the sodium ions associated with the particle surface sulfate ions (derived from the persulfate

Table 1 Some experimental data obtained from the ST miniemulsion polymerizations stabilized by 5 mM SDS and various levels of dye

	[dye] (%)	$d_{m,i}$ (nm)	$N_{m,i} \times 10^{-15}$ (1/l-H ₂ O)	$d_{p,f}$ (nm)	$N_{p,f} \times 10^{-17}$ (1/l-H ₂ O)	$N_{p,f}/N_{m,i}$	X_t (%)	P_{dye} (%)
MP1	0.1	719	1.427	107	3.580	250.8	81.8	56.2
MP2	0.5	641	2.013	104	3.809	189.2	81.4	58.7
MP3	1.0	872	0.559	96	4.750	850.0	79.0	65.8

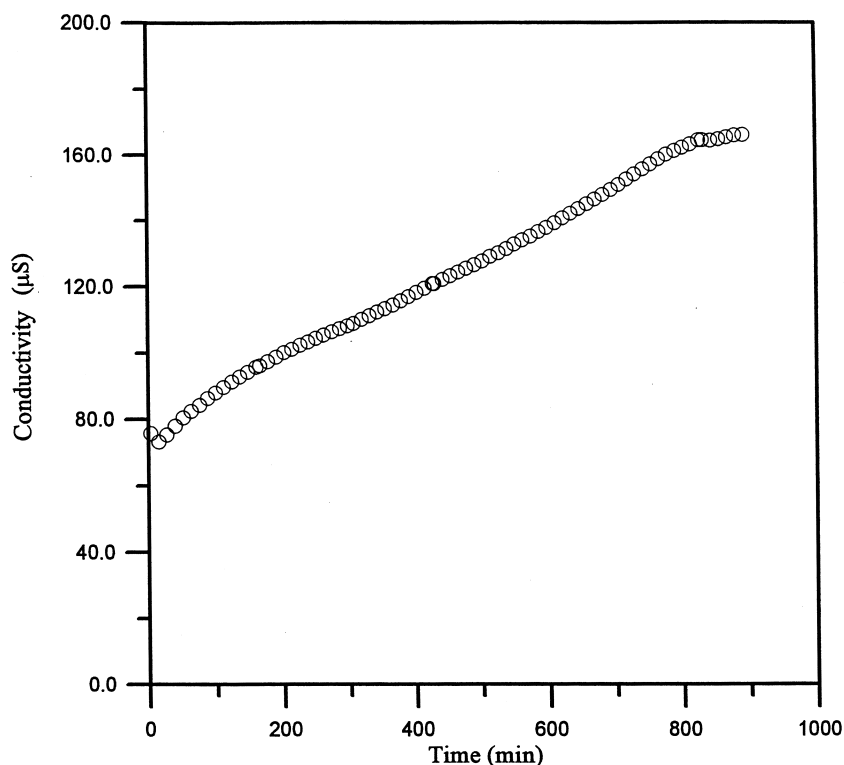


Figure 8 Relative conductivity as a function of time for the homogenized ST miniemulsion stabilized by 5 mM SDS only

initiator) may also contribute to the decreased conductivity. The point at which the minimal conductivity occurs marks the end of particle nucleation originated from the aqueous phase.

After the minimal conductivity point is reached, the oligomeric radicals produced in the aqueous phase may either enter the existing latex particles or penetrate the remaining monomer droplets to convert them into latex particles. Furthermore, the growing latex particles may compete with the monomer droplets for monomer and surfactant. Consumption of monomer in the latex particles will cause the monomer molecules to diffuse from the monomer droplets to these reaction loci, even though the hydrophobic dye in the monomer droplets offers resistance against such a mass transfer process. The adsorbed surfactant may be released from the shrinking monomer droplet surfaces and, thereby, increase the conductivity in the aqueous phase. Diffusional degradation of the monomer droplets may also reduce the monomer droplet-water interfacial area and hence contribute to the increased conductivity. To demonstrate the effect of Ostwald ripening on the relative conductivity profile, the following experiment was carried out. The mixture comprising H₂O, 5 mM SDS and 24.24% ST based on total water was homogenized first by the microfluidizer operated at 5000 psi outlet pressure and 10 passes and then allowed to stand at room temperature for the conductivity measurements. The blue dye was not used in this experiment in order to facilitate the diffusional degradation of the monomer droplets. Indeed, the relative conductivity continues to rise within an observation period of 900 min, presumably due to the Ostwald ripening effect (see Figure 8). The maximal point occurring at $X \sim 80\%$ (see Figures 5 and 7) marks the disappearance of the monomer droplets. Subsequently, the relative conductivity starts to decrease and then level off toward the end of polymerization owing to the depletion of surfactant and perhaps initiator in water.

Conventional ST emulsion polymerization in the presence of dye

There is no doubt that the osmotic pressure effect plays an important role in stabilizing the ST miniemulsions. This osmotic pressure can be detected indirectly by retardation of the diffusional degradation of the monomer droplets in the shelf-life experiment. It was postulated that conventional emulsion polymerization of styrene in the presence of a water-insoluble dye also can be used to measure the osmotic pressure exerted on the reaction system. The rationale of this speculation is briefly discussed below. First, the monomer droplets produced by a typical mechanical agitator operated at 400 rpm are quite large ($d_m > 10^3$ nm). According to equation (1), the water solubility of monomer in these monomer droplets decreases rapidly with an increase in the droplet size ($C(d_m) \sim \exp(-d_m^{-1})$). This may greatly reduce the

extent of Ostwald ripening. Moreover, these monomer droplets have rather limited oil-water interfacial area and they are not effective in capturing the oligomeric radicals from the aqueous phase. As a result, the latex particles are most likely generated via homogeneous nucleation if the surfactant concentration is below its CMC. These growing latex particles then require the supplies of monomer from the monomer droplets, which only serve as a monomer reservoir in this case. However, the hydrophobic dye uniformly distributed in the monomer droplets offers significant resistance to the transport of monomer from the monomer droplets, across the aqueous phase, and then to the latex particles. This may greatly reduce the monomer concentration in the latex particles and, therefore, slow down the propagation reaction. The rate of polymerization is proportional to the monomer concentration in the latex particles ($[M]_p$), the average number of free radicals per particle (\bar{n}) and the number of latex particles per unit volume of water (N_p). It is postulated that in the constant polymerization rate region N_p and \bar{n} are not dependent on [dye] ranging from 0% to 1%. The validity of this assumption will be examined later in this paper. Thus, the influence of [dye] on the polymerization rate, if present, is closely related to changes in $[M]_p$ with [dye]. Under the circumstances, the relative reduction in the rate of polymerization ($|R_p - R_{p0}|/R_{p0}$) may be used as an indicator for the extent of the osmotic pressure effect. The parameters R_p and R_{p0} represent the rate of polymerization (determined from the linear portion of the X versus t data) for the conventional emulsion polymerization of styrene with and without dye, respectively.

A series of conventional emulsion polymerization of styrene in the presence of dye was then carried out to verify the above idea. The SDS concentration was kept constant at 5 mM, whereas [dye] was varied between 0% and 1% in this series of experiments. The data of X and relative conductivity as a function of t are shown in Figures 9 and 10, respectively. The data of the rate of polymerization (R_p , determined from the linear portion of the X versus t curve shown in Figure 9), the monomer conversion at the end of polymerization (X_f), the latex particle size at the end of polymerization ($d_{p,f}$), the number of latex particles at the end of polymerization ($N_{p,f}$), and the weight percentage of dye that has been incorporated into the final latex particles (P_{dye}) are compiled in Table 2. Note that the values of $N_{p,f}$ for EP3, EP4 and EP5 were not determined since monomer droplets are most likely present in the reaction system due to the relatively low levels of X_f (36%–45%). The presence of large monomer droplets ($> 10^3$ nm in diameter) may cause a significant error in the particle size measurements using the dynamic light scattering technique and, thereby, result in unreliable $N_{p,f}$ data. The values of $N_{p,f}$ seem to be insensitive to changes in [dye] (see the $N_{p,f}$ data for EP1, EP2, and EP6 in Table 2). This result implies that N_p determined in the

Table 2 Some experimental data obtained from the conventional ST emulsion polymerizations in the presence of various levels of [dye]

	EP1	EP2	EP3	EP4	EP5	EP6
[dye] (%)	0.00	0.015	0.05	0.10	0.50	1.00
$R_p \times 10^3$ (mol/l/min)	6.54	4.52	3.82	2.98	3.13	6.61
$ R_p - R_{p0} /R_{p0}$	0.00	0.31	0.42	0.54	0.52	0.01
$d_{p,f}$ (nm)	214	222	277	272	297	232
X_f (%)	77.1	52.0	45.3	35.7	36.8	75.0
$N_{p,f} \times 10^{-16}$ (1/l-H ₂ O)	4.650	4.324				3.661
P_{dye} (%)	0.0	1.1	2.1	1.7	5.0	4.2

constant reaction rate region does not change significantly when [dye] increases from 0% to 1%. Furthermore, the amount of dye incorporated into the monomer-swollen polymer particles is rather limited ($[dye] P_{dye} \leq 420$ ppm

based on total monomer). Therefore, the influence of dye on \bar{n} is probably negligible because most of the dye molecules are located in the monomer droplets during polymerization. For conventional emulsion polymerization of styrene in the

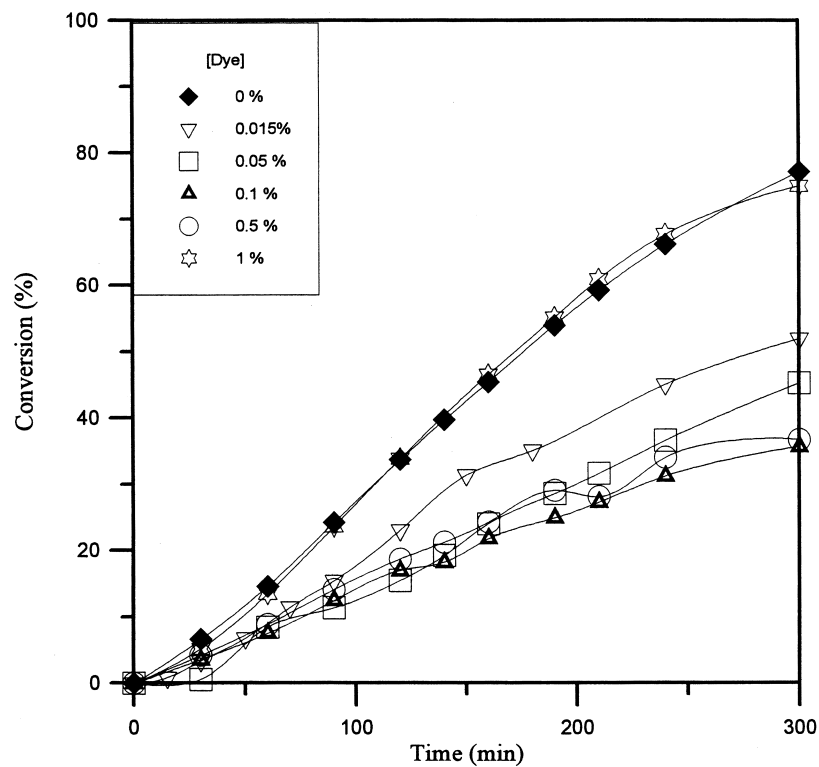


Figure 9 Monomer conversion as a function of time for conventional emulsion polymerization of styrene stabilized by 5 mM SDS. [dye] = (◆) 0, (▽) 0.015, (□) 0.05, (△) 0.1, (○) 0.5, (★) 1.0 wt%

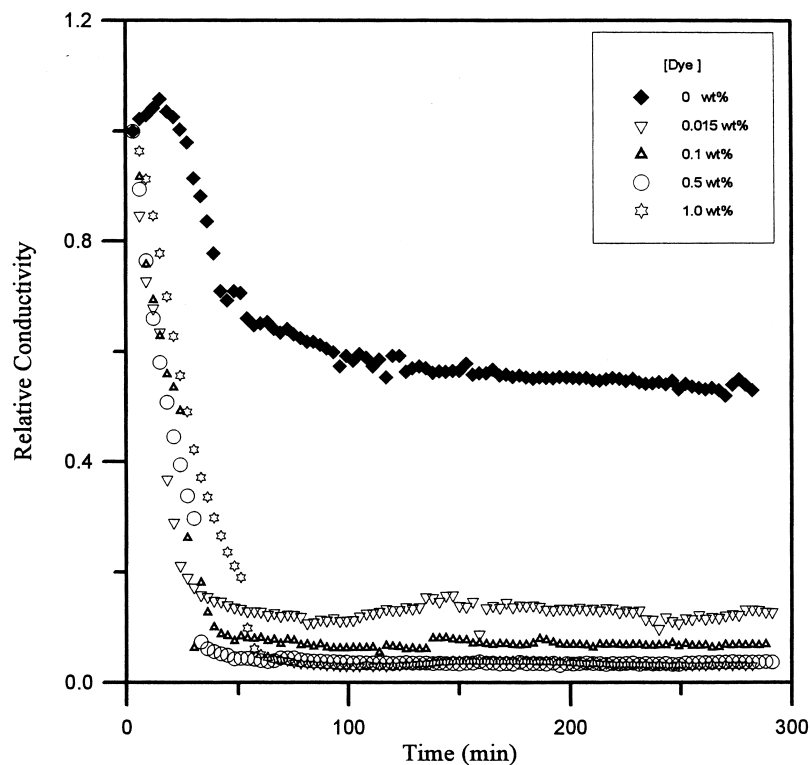


Figure 10 Relative conductivity as a function of time for conventional emulsion polymerization of styrene stabilized by 5 mM SDS. [dye] = (◆) 0, (□) 0.05, (△) 0.1, (○) 0.5, (★) 1.0 wt%

constant reaction rate region, the value of \bar{n} is equal to 0.5 due to the effective segregation of free radicals in a large number of growing latex particles (Smith–Ewart case II kinetics)². Thus, it seems reasonable to assume that in the constant polymerization rate region the values of N_p and \bar{n} are not dependent on [dye] and the only influence of the dye molecules on the reaction kinetics is the retarded diffusion of monomer from the monomer droplets to the growing latex particles.

The R_p data are in the range of 2.98×10^{-3} – 6.61×10^{-3} mol/l/min, which is about one order of magnitude smaller than those for the ST miniemulsion polymerizations stabilized by 5 mM SDS and various levels of [dye]. This is probably due to the fact that the SDS concentration is below its CMC. Therefore, the number of latex particles nucleated in the aqueous phase may be smaller than that of the miniemulsion polymerization. A reduction in the number of reaction loci may thus result in a lower R_p . Interestingly enough, R_p first decreases to a minimum when [dye] increases from 0% to 0.1% (see Figure 9 and Table 2). Further increasing [dye] then causes R_p to go up significantly. The data of P_{dye} as a function of [dye] listed in Table 2 indicate that approximately 1%–5% of the monomer droplets can be successfully transformed into the latex particles during polymerization. In addition, P_{dye} increases as [dye] is increased from 0% to 1.00%. This trend then implies that the higher the [dye], the more important is the monomer droplet nucleation. The value of $|R_p - R_{p0}|/R_{p0}$ increases from 0.31 to 0.54 when [dye] increases from 0.015% to 0.10% (see Table 2). In this case, monomer droplet nucleation is not important ($P_{\text{dye}} \leq 2\%$) and the increased $|R_p - R_{p0}|/R_{p0}$ is simply attributed to the increased osmotic pressure with [dye]. However, monomer droplet nucleation becomes significant ($P_{\text{dye}} \sim 5\%$) and the value of $|R_p - R_{p0}|/R_{p0}$ is greatly reduced to the level of 0.01 for the polymerization with [dye] = 1%.

For the conventional emulsion polymerizations, the relative conductivity versus t curves shown in Figure 10 are quite different from those for the miniemulsion polymerizations (see Figure 7). As shown in Figure 10, nucleation of primary particles in the aqueous phase is responsible for the rapidly decreased conductivity during the early stage of polymerization. Comparing Figures 9 and 10 shows that formation of primary particles stops at a monomer conversion of 10% or lower, which is typical of the conventional emulsion polymerization stabilized by a relatively low level of surfactant. This result again suggests that monomer droplet nucleation is not the dominating mechanism for the conventional emulsion polymerization of styrene in the presence of dye. It is also interesting to note that the relative conductivity decreases significantly when a small amount of dye is added to the reaction system. This is probably caused by the retarded monomer diffusion from the monomer droplets to the growing latex particles, provided by incorporating the very hydrophobic dye into the monomer droplets. The relatively stable monomer droplets tend to retain the adsorbed surfactant molecules and only contribute a little to the supply of ionic species in water.

So far, the authors have demonstrated the feasibility of using the hydrophobic low molecular weight blue dye as the cosurfactant to prepare relatively stable ST miniemulsions. Furthermore, the blue dye may serve as a probe for determination of the fraction of the original monomer droplets nucleated during the subsequent miniemulsion polymerization. For the miniemulsion polymerization

stabilized by a more effective cosurfactant (e.g. HD, SMA, DMA or CA), incorporation of a small amount of dye into the monomer droplets in combination with conductivity measurements should be a powerful tool to investigate the related particle nucleation mechanisms. Further research on this subject is in progress in our laboratory.

CONCLUSIONS

The water-insoluble, low molecular weight dye (Blue 70) offers resistance to diffusional degradation of the monomer droplets with a relatively broad droplet size distribution (Ostwald ripening). After sufficient homogenization, relatively stable styrene (ST) miniemulsions were prepared by using 5 mM sodium dodecyl sulfate (SDS) and various levels of dye ([dye] = 0.1–1.0% based on total monomer). The average monomer droplet size (d_m) increases gradually and then levels off for these miniemulsions aged at 35°C, which is attributed to the competition between the Ostwald ripening and osmotic pressure effects. The Ostwald ripening rate decreases with increasing [dye]. The miniemulsions also exhibit significant creaming upon aging at 35°C. Judging from these shelf-life data, the blue dye is not as effective as the cosurfactants CA and DMA in stabilizing the ST miniemulsions.

In the ST miniemulsion polymerizations stabilized by SDS/dye, the average size of the latex particles/monomer droplets (d) decreases rapidly to a minimum, followed by a gradual increase to the plateau during the reaction. The rapidly decreased d with t is caused by the production of particle nuclei via homogeneous nucleation. Approximate 60% of the monomer droplets initially present in the reaction system was successfully nucleated during polymerization based on the data of the weight percentage of dye incorporated into the final latex particles (P_{dye}). The parameter P_{dye} goes up with increasing [dye]. This is attributed to the increased resistance against diffusional degradation of the monomer droplets. This may greatly reduce the number of primary particles nucleated in the aqueous phase and, thereby, increase the degree of incorporation of dye into the final latex particles. The conductivity data collected during polymerization also supports the mixed modes of particle nucleation.

Finally, a series of conventional ST emulsion polymerizations stabilized by 5 mM SDS was carried out to study the influence of dye ([dye] = 0.015%–1.00%) on the mass transfer of monomer from the monomer droplets to the growing latex particles (reaction loci). The P_{dye} data show that only 1%–5% of the original monomer droplets can be successfully transformed into the latex particles during polymerization. In addition, P_{dye} increases with increasing [dye]. This trend then implies that the higher the [dye], the more important is the monomer droplet nucleation. The relative reduction in the polymerization rate ($|R_p - R_{p0}|/R_{p0}$) increases from 0.31 to 0.54 when [dye] increases from 0.015% to 0.10%. In this case, monomer droplet nucleation is not important ($P_{\text{dye}} \leq 2\%$) and the increased $|R_p - R_{p0}|/R_{p0}$ is simply attributed to the increased osmotic pressure with [dye]. This may greatly reduce the monomer concentration in the latex particles and, thereby, slow down the propagation reaction. On the other hand, a rapidly decreased $|R_p - R_{p0}|/R_{p0}$ is observed for the polymerization with [dye] = 1% due to the increased importance of the monomer droplet nucleation. For the conventional emulsion polymerization in which homogeneous nucleation is

dominating, the relative conductivity versus t profiles are quite different from those for the miniemulsion polymerizations

ACKNOWLEDGEMENTS

This work was supported by the National Science Council of Taiwan, Republic of China.

REFERENCES

1. Harkins, W.D., *Journal of American Chemistry Society*, 1947, **69**, 1428.
2. Smith, W.V. and Ewart, R.W., *Journal of Chemistry and Physics*, 1948, **16**, 592.
3. Smith, W.V., *Journal of American Chemistry Society*, 1948, **70**, 3695.
4. Roe, C.P., *Industrial Engineering Chemistry*, 1968, **60**, 20.
5. Fitch, R.M., Prenosil, M.B. and Sprick, K.J., *Journal of Polymer Science*, 1969, **C 27**, 95.
6. Hansen, F.K. and Ugelstad, J., *Journal of Polymer Science, Polymer Chemistry Edition*, 1978, **16**, 1953.
7. Fitch, R.M. and Watson, R.C.J., *Journal of Colloid Interface Science*, 1979, **68**, 14.
8. Lichti, G., Gilbert, R.G. and Napper, D.H., *Journal of Polymer Science, Polymer Chemistry Edition*, 1983, **21**, 269.
9. Song, Z. and Poehlein, G.W., *Journal of Macromolecular Science and Chemistry*, 1988, **A 25**, 403.
10. Song, Z. and Poehlein, G.W., *Journal of Macromolecular Science and Chemistry*, 1988, **A 25**, 1587.
11. Ugelstad, J., El-Aasser, M.S. and Vanderhoff, J.W., *Polymer Letters*, 1973, **11**, 503.
12. Ugelstad, J., Hansen, F.K. and Lange, S., *Die Makromolekular Chemische*, 1974, **175**, 507.
13. Durbin, D.P., El-Aasser, M.S., Sudol, E.D. and Vanderhoff, J.W., *Journal of Applied Polymer Science*, 1979, **24**, 703.
14. Chamberlain, B.J., Napper, D.H. and Gilbert, R.G., *Journal of the Chemistry Society, Faraday Transactions*, 1982, **78**, 591.
15. Choi, Y.T., El-Aasser, M.S., Sudol, E.D. and Vanderhoff, J.W., *Journal of Polymer Science, Polymer Chemistry Edition*, 1985, **23**, 2973.
16. Delgado, J., El-Aasser, M.S. and Vanderhoff, J.W., *Journal of Polymer Science, Polymer Chemistry Edition*, 1986, **24**, 861.
17. Delgado, J., El-Aasser, M.S., Silebi, C.A., Vanderhoff, J.W. and Guillot, J.W., *Journal of Polymer Science, Polymer Chemistry Edition*, 1988, **26**, 1495.
18. Delgado, J., El-Aasser, M.S., Silebi, C.A., Vanderhoff, J.W. and Guillot, J., *Journal of Polymer Science, Polymer Chemistry Edition*, 1989, **27**, 193.
19. Rodriguez, V.S., El-Aasser, M.S., Asua, J.M. and Silebi, C.A., *Journal of Polymer Science, Polymer Chemistry Edition*, 1989, **27**, 3659.
20. Tang, P.L., Sudol, E.D., Silebi, C.A. and El-Aasser, M.S., *Journal of Applied Polymer Science*, 1991, **43**, 1059.
21. Pan, Z.R., Fan, H., Weng, Z.X. and Huang, Z.M., *Polymer International*, 1993, **30**, 259.
22. Alduncin, J.A., Forcada, J. and Asua, J.M., *Macromolecules*, 1994, **27**, 2256.
23. Miller, C.M., Sudol, E.D., Silebi, C.A. and El-Aasser, M.S., *Journal of Polymer Science, Polymer Chemistry Edition*, 1995, **33**, 1391.
24. Kabalnov, A.S. and Shchukin, E.D., *Advances in Colloid Interface Science*, 1992, **38**, 69.
25. Chern, C.S. and Chen, T.J., *Colloid Polymer Science*, 1997, **275**, 546.
26. Chern, C.S. and Chen, T.J., *Colloid Polymer Science*, 1997, **275**, 1060.
27. Reimers, J.L. and Schork, F.J., *Journal of Applied Polymer Science*, 1996, **60**, 251.
28. Chen, T.J., M.Sc. Thesis, National Taiwan Institute of Technology, Taiwan, 1997.
29. Rehfeld, S.J., *Journal of Physics and Chemistry*, 1967, **71**, 738.